Laboratori Nazionali di Frascati

LNF-74/21(P)

L. Bergamo, B. D'Ettorre Piazzoli, P. Picchi and R. Visentin:

# THE NEUTRINO DIFFERENTIAL CROSS-SECTION ($d\sigma/dQ^2$) PREDICTIONS AS A FUNCTION OF INTERMEDIATE BOSON (W) MASS

Lett. Nuovo Cimento 9, 224 (1974)

LETTERE AL NUOVO CIMENTO VOL. 9, N. 6 9 Febbraio 1974

# The Neutrino Differential Cross-Section ($d\sigma/dQ^2$) Predictions as a Function of Intermediate Boson (W) Mass.

L. BERGAMASCO and B. D'ETTORRE PIAZZOLI

*Laboratorio di Cosmogeofisica del CNR - Torino*

P. PICCHI

*Scuola di Perfezionamento in Fisica Cosmica dell'Università - Torino*
*Laboratori Nazionali di Frascati del CNEN - Frascati*

R. VISENTIN

*Laboratori Nazionali di Frascati del CNEN - Frascati*

(ricevuto il 30 Luglio 1973)

In the present study on the weak interactions there is the problem of finding an intermediary of the weak force. The simplest possibility lies in the existence of one or more intermediate bosons W. Activity to discover such a particle is enormous.

The Batavia National Laboratories accelerator will permit experiments with neutrinos of energy up to 500 GeV, and one of the detectors will be a big bubble chamber filled with hidrogen, deuterium or neon (1).

In this work we give the differential cross-section $d\sigma/dQ^2$ for the interactions of neutrinos (2) at energies $E_\nu = 100$, 200, 500 GeV on Ne nuclei calculated for different values of $M_W$.

The measurements of $d\sigma/dQ^2$ with bubble chambers are rather simple, demanding only the identification of the prompt negative muon and the value of its momentum and scattering angle. These data may be very useful if the W decay into hadrons is dominant (3).

The reactions which we have considered are the following:

(1) $\nu + \mathrm{Ne} \to \mu^- + \mathrm{h}$ (virtual W),

(2) $\nu + \mathrm{Ne} \to \mu^- + \mathrm{W}^+ + \mathrm{h}$ (real W),

(1) C. BALTAY: *Neutrino physics in a large bubble chamber at very high energies*, in *Proceedings of the Joint Japanese-U.S. Seminar on Elementary Particle Physics with Bubble Chamber Detectors*, SLAC-144 (1972).

(2) At NAL the $\bar{\nu}$ fluxes are about a factor of 3 less than the $\nu$ fluxes of ref. (1).

(3) D. CLINE, A. K. MANN and C. RUBBIA: *Phys. Rev. Lett.*, **25**, 1309 (1970).

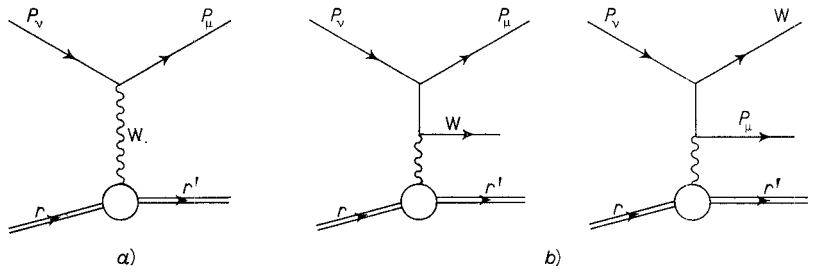


Fig. 1. – *a*) The diagram of virtual-W production by neutrinos, *b*) the diagram of real-W production by neutrinos.

where W is the usual spin-one W-boson and h the hadronic final state. To the lowest order of perturbation theory these processes are represented by the diagrams of Fig. 1, where

$P_\nu$ = four-momentum of the neutrino,
$P_\mu$ = four-momentum of the muon,
$r$ = four-momentum of the initial hadronic state,
$r'$ = four-momentum of the final hadronic state,
$Q = P_\nu - P_\mu$ = four-momentum transferred from leptons to hadrons and W.

We define moreover:

$s = r - r'$ = four-momentum transferred to the hadronic vertex (for process (1) $Q = s$),
$\nu = E_\nu - E_\mu$ = energy transferred from leptons to hadrons and to W,
$\nu_h = E_{r'} - E_r$ = energy transferred to the hadronic vertex (for process (1) $\nu_h = \nu$),
$M_N$ = the nucleon mass,
$M_A$ = the mass of the hadronic initial state (nucleon or nucleus),
$M_W$ = the W-boson mass,
$\varphi$ = the azimuthal angle of the final-hadronic-state momentum around $\boldsymbol{Q}$.

The basic formula (which gives the cross-section $\nu$-nucleon) for reaction (1), Fig. 1*a*), is

$$(3) \qquad \frac{d^2\sigma^\pm}{d\nu\, dQ^2} = \frac{G^2}{4\pi}\frac{1}{E_\nu^2}\left[Q^2 W_1^\pm + \left(2E_\nu^2 - 2E_\nu\nu - \frac{Q^2}{2}\right)W_2^\pm \mp W_3^\pm \frac{2E_\nu - \nu}{2M_N}Q^2\right]\frac{1}{(1+Q^2/M_W^2)^2},$$

where $G = 1.02\, M_p^{-2}\cdot 10^{-5}$ is the Fermi coupling constant ($M_p$ = proton mass).

$W_{1,2,3}^\pm$ are the form factors describing the process (the plus or minus sign refers respectively to neutrino or antineutrino). In the evaluation of eq. (3) we assume [4] scale invariance to hold for $W_1^\pm$.

---

[4] C. CASTAGNOLI, E. ETIM and P. PICCHI: *Lett. Nuovo Cimento*, **4**, 564 (1970).

The total ν-nucleon cross-section results for $M_W = \infty$

$$\sigma_{\nu\text{nucleon}} = \frac{\sigma_{\nu p} + \sigma_{\nu n}}{2} = 0.68 \cdot 10^{-38} E_\nu \text{ cm}^2$$

are in good agreement with the CERN experimental results $\sigma_{\nu\text{nucleon}} = (0.69 \pm 0.14) \cdot 10^{-38} E_\nu \text{ cm}^2$ for $E_\nu < 10$ GeV.

Reaction (2) (see Fig. 1*b*)) represents the W direct production by neutrinos (to lowest order the cross-section for $\bar{\nu}$ is identical).

For a target of charge $Z$ at rest we have

$$\frac{\mathrm{d}^2\sigma_W}{\mathrm{d}Q^2\,\mathrm{d}\nu} = \frac{Z^2\alpha^2}{(2\pi)^2} g^2 \frac{1}{E_\nu^2 M_A} \frac{1}{|\boldsymbol{Q}(Q^2, \nu)|} \int_{s^2_{\min}}^{s^2_{\max}} \frac{\mathrm{d}s^2}{s^4} \mathscr{F}(Q^2, \nu, s^2)\,, \tag{4}$$

where $\alpha$ is the fine-structure constant 1/137 and $g^2 = (M_W^2/\sqrt{2})G$ is the semi-weak coupling constant.

The function $\mathscr{F}(Q^2, \nu, s^2)$ is given explicitly after the analytical evaluation of the integral:

$$\mathscr{F}(Q^2, \nu, s^2) = \frac{1}{2M_A} \int_0^{2\pi} T_{\mu\nu} W_{\mu\nu}\,\mathrm{d}\varphi\,. \tag{5}$$

The tensor $T_{\mu\nu}$ which arises after summation over the lepton spins and W polarizations represents the semi-weak and electromagnetic vertex. The hadronic vertex is described in the usual way by the tensor $W_{\mu\nu}$:

$$W_{\mu\nu} = -W_1(s^2)\left(\delta_{\mu\nu} - \frac{s_\mu s_\nu}{s^2}\right) + \frac{W_2(s^2)}{M_A^2}\left(r_\mu - \frac{rs}{s^2} s_\mu\right)\left(r_\nu - \frac{rs}{s^2} s_\nu\right), \tag{6}$$

where for *incoherent production on nucleon* we use

$$W_1(s^2) = \tfrac{1}{2} s^2 G_M^2\,, \qquad W_2(s^2) = 2M_A^2(1+\tau)^{-1}(G_E^2 + \tau G_M^2)\,,$$

$$\tau = \frac{-s^2}{4M_N}\,.$$

$$G_E(\text{proton}) = G_M(\text{proton})/2.79 = -G_M(\text{neutron})/1.91 = \left(1 - \frac{-s^2}{0.71}\right)^{-2},$$

$$G_E(\text{neutron}) = 0\,,$$

while for *coherent production on nucleus* we have

$$W_1(s^2) = 0\,, \qquad W_2(s^2) = 2M_A^2 |F(s^2)|^2\,, \qquad F(s^2) = \exp\left[\frac{s^2 a^2}{6}\right]$$

with

$$a = 5.1\, A^{\frac{1}{3}} (\text{GeV/c})^{-1}\,.$$

For the inelastic channel (the cross-section on nucleon is about $\frac{1}{2}$ of the incoherent cross-section on proton) the structure functions are quite different and depend on $\nu_h$.

Assuming the scaling behaviour of $\nu_h W_2(s^2, \nu_h)$, we have [5]

$$W_1(s^2, \nu_h) = \left(1 + \frac{\nu_h^2}{s^2}\right) \frac{W_2(s^2, \nu_h)}{1 + R},$$

$$W_2(s^2, \nu_h) = \frac{M_\mathcal{N}}{\nu_h} F(x), \qquad F(x) = 0.4 \frac{1 - \exp[-(x-1)]}{1 + x/20},$$

with

$$\nu_h = \frac{1}{2M_\mathcal{N}} (-s^2 + M_B^2 - M_\mathcal{N}^2),$$

$$x = \frac{-2M_\mathcal{N}\nu_h}{s^2},$$

$$R = \sigma_L/\sigma_T \simeq 0.$$

$M_B^2 = r'^2$ is the squared mass of the hadronic final state.

After saturation, the explicit form of $T_{\mu\nu} W_{\mu\nu}$ depends on $Q^2$, $\nu$, $s^2$ and on rational functions of the powers (up to the second) of $\cos\varphi$: it follows that $\mathscr{F}(Q^2, \nu, s^2)$ can be easily given in closed form.

The calculation of $d\sigma/dQ^2$ requires only two numerical integrations over $\nu$ (between $\nu_{\min}(Q^2)$ and $\nu_{\max}(Q^2)$) and $s^2$.

For the inelastic channel we must carry out a further integration over the squared mass of the final hadronic state:

$$\frac{d\sigma_W^{in}}{dQ^2} = \int_{r'^2_{\min}}^{r'^2_{\max}} \frac{d\sigma_W}{dQ^2 dr'^2} r'^2 dr'^2.$$

All integration limits are unambiguously defined analitically. We have checked the validity of the calculations by integrating the differential cross-section over $Q^2$. The total cross-sections (with the anomalous magnetic moment of the W $K = 0$) agree to within 5% with those of ref. [5].

The differential cross-section per proton on a neon target is

$$\frac{d\sigma}{dQ^2}\Big/\text{proton} = \frac{d\sigma^+}{dQ^2}(\text{proton}) + \frac{A-Z}{Z}\frac{d\sigma^+}{dQ^2}(\text{neutron}) +$$

$$+ \frac{d\sigma_W}{dQ^2}(\text{proton}) + \frac{A-Z}{Z}\frac{d\sigma_W}{dQ^2}(\text{neutron}) + \frac{1}{Z}\left(1 - \frac{1}{Z}\right)\frac{d\sigma_W}{dQ^2}(\text{coherent}) +$$

$$+ \frac{d\sigma_W^{in}}{dQ^2}(\text{proton}) + \frac{A-Z}{Z}\frac{d\sigma_W^{in}}{dQ^2}(\text{neutron}).$$

In our calculations we assume equal the proton and neutron inelastic cross-sections for W production, and we do not include corrections for the Fermi motion and the Pauli principle.

---

[5] R. W. BROWN and J. SMITH: *Phys. Rev. D*, **3**, 207 (1971).

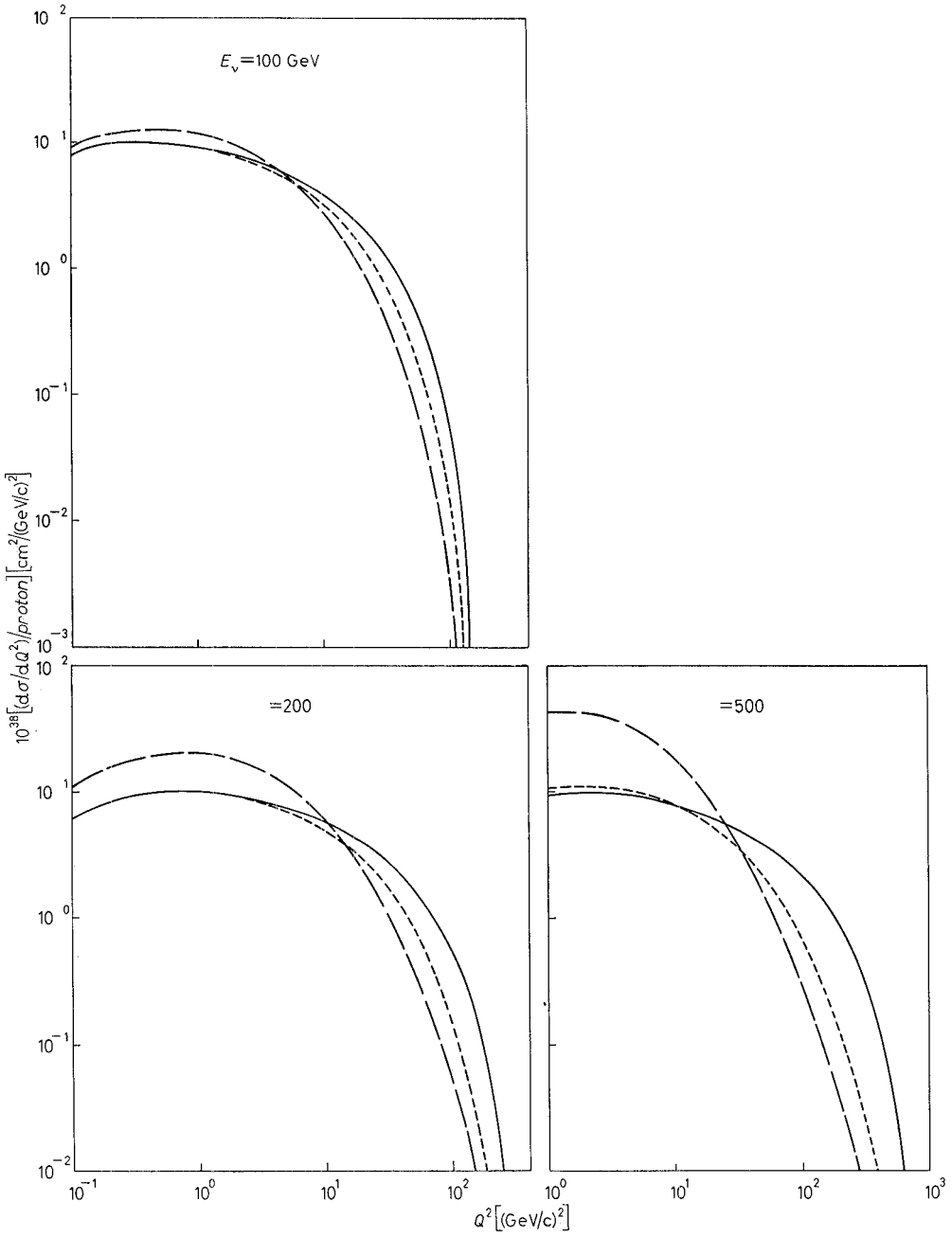


Fig. 2. – Inelastic neutrino $(d\sigma/dQ^2)$/proton for $E_\mu > 1.5$ GeV. $M_W = \infty$ (full lines), $M_W = 10$ GeV (dashed lines), $M_W = 5$ GeV (long-dashed lines).

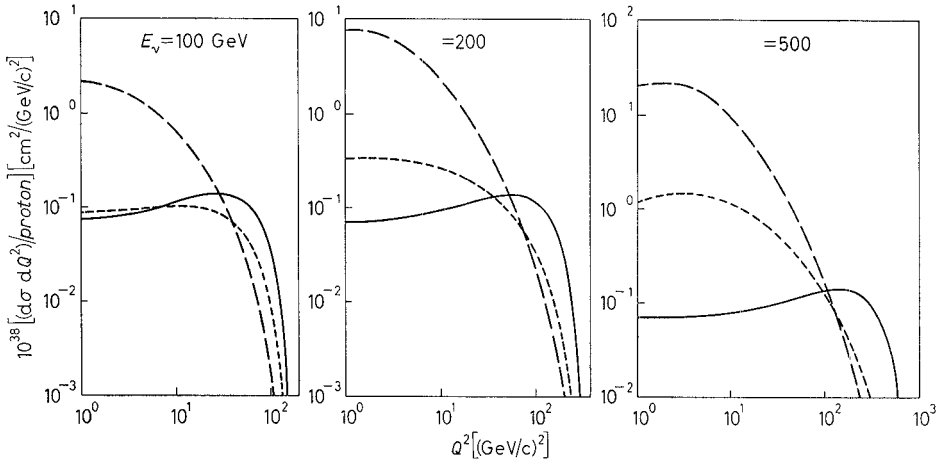


Fig. 3. – Inelastic neutrino ($d\sigma/dQ^2$)/proton for $1.5 < E_\mu < 0.15 E_\nu$ GeV. $M_W = \infty$ (full lines), $M_W = 10$ GeV (dashed lines), $M_W = 5$ GeV (long-dashed lines).

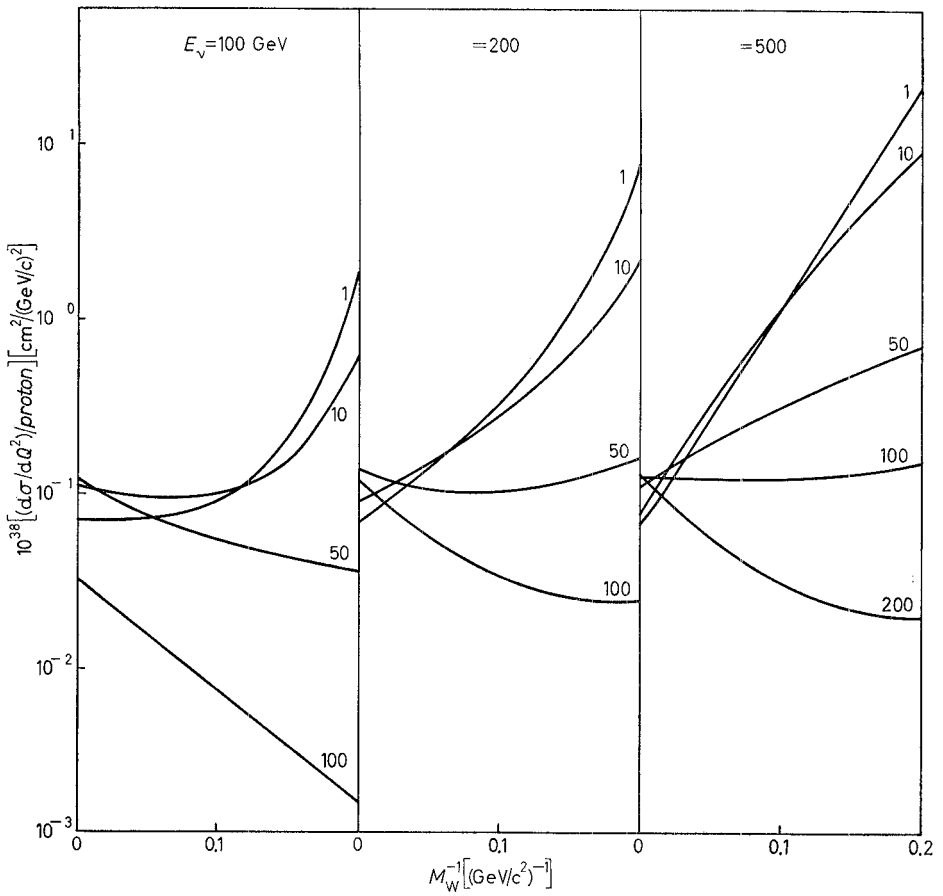


Fig. 4. – Inelastic neutrino ($d\sigma/dQ^2$)/proton for different $Q^2$ values (1, 10, 50, 100, 200) as a function of $M_W^{-1}$.

In Fig. 2 we give $(d\sigma/dQ^2)$/proton for $E_\mu > 1.5$ GeV and $M_W = \infty$, 10, 5 GeV (6). For $Q^2 \leqslant 20$ (GeV/c)$^2$ and for masses $M_W \geqslant 10$ GeV there are no peculiar differences.

In Fig. 3 we show $(d\sigma/dQ^2)$/proton for $1.5 < E_\mu < 0.15 E_\nu$ GeV and $M_W = \infty$, 10, 5 GeV. These curves are sharply different, even for low $Q^2$. This difference results (3) from the fact that in process (2) a large energy transfer to real W is accompanied by a low $Q^2$.

The conclusions which may be drawn are synthetized in Fig. 4, which shows $(d\sigma/dQ^2)$/ /proton for different $Q^2$ values (1, 10, 50, 100, 200) as a function of $M_W^{-1}$, namely

ratios between different $Q^2$ are very sensible to $M_W$,

also for $E_\nu = 100$ GeV it is possible to carry out experimental measurements which can evidence masses $M_W$ of about $(15 \div 20)$ GeV.

---

(6) The basic idea to identify the muon is to use slabs of great thickness which absorb the hadronic component. The eventual cut-off $E_\mu > 1.5$ GeV corresponds to the muon energy loss through the medium.